Cell, Volume *135*

Supplemental Data

Systematic Genetic Analysis of Virulence in the Human Fungal Pathogen *Cryptococcus neoformans*

Oliver W. Liu, Cheryl D. Chun, Eric D. Chow, Changbin Chen, Hiten D.Madhani, and Suzanne M. Noble

SUPPLEMENTAL FIGURE LEGENDS AND FIGURES

Figure S1

In vitro growth defects correlate with *in vivo* infectivity defects. Enrichment for mutants with infectivity defects for a given YNB growth score (growth at 37°C in minimal medium) was determined using a 25-mutant moving average across growth scores and a hypergeometric test. The red-dotted line indicates the cutoff used to identify significant growth defects.

Figure S2

Predicted structures of proteins encoded by genes discussed in this work. Predicted protein domains were identified using SMART (see Supplementary Experimental Procedures).

Figure S3

Identification and verification of genes involved in mutant phenotypes. Linkage of observed phenotypes and the expected gene deletions was confirmed by reconstructing 107 independent gene knockout strains and retesting for the original phenotypes. **(A)** 67 reconstructed knockout mutants were retested by STM and confirmed to reproduce (blue dots) or not to reproduce (red dots) infectivity phenotypes. The blue line shows the correlation of STM scores of original and reconstructed knockouts that reproduced the expected phenotype. **(B)** Capsule defects in both the original and reconstructed *cpl1Δ* mutant strains were verified by India ink staining under capsule-inducing and non-inducing growth conditions. **(C)** Melanin phenotypes in both the original and reconstructed mutant strains were verified by growth at 30°C on plates containing L-DOPA. *rco1Δ* displayed no melanin defect. *ssn801Δ* displayed an increase in melanization. The remaining mutant strains shown in this figure displayed defects in melanization **(D)** Summary of phenotype retesting by knockout reconstruction.

Figure S4

Deletion of *SET3* and *HOS2* results in enlarged capsules. **(A)** The capsules of wild-type and *set3Δ* and *hos2Δ* mutant strains grown under capsule-inducing conditions were directly visualized by India ink staining. *set3Δ* and *hos2Δ* cells are slightly larger than wild-type. **(B)** The sizes of these capsules were quantified relative to the diameters of the cells. Capsules from at least 30 cells per strain were measured. Error bars represent the SD.

Figure S5

Growth on acidified nitrite and pH 4 medium. **(A)** Serial dilutions of wild-type (WT) and mutant strains were grown on pH 4 YPAD agar and pH 4 YPAD agar containing 2 mM $NaNO_2$. A mutant containing a deletion of the flavohemoglobin gene (*fhb1Δ*) was used as a positive control for NO sensitivity. Red boxes indicate mutants that displayed sensitivity to acidified nitrite. These phenotypes were confirmed in repeated independent experiments (data not shown). Asterisks indicate strains that displayed potential growth defects on pH 4 medium in general. **(B)** Mutants that displayed potential growth defects on pH 4 medium were retested on pH 4 and pH 7 media using individually-grown 5mL starting cultures. A mutant containing a deletion of the inositol phosphosphingolipid-phospholipase C1 gene (*isc1Δ*) was used as a positive control for pH 4 sensitivity. Neither of the mutants displayed discernible growth defects on pH 4 medium upon retest.

Figure S6

Sensitivity to SDS. Serial dilutions of wild-type (WT) and mutant strains were grown on YPAD plates and YPAD plates containing 0.03% SDS. Red boxes indicate mutants that displayed sensitivity to SDS.

Figure S7

Mutants containing deletions of *SRE1*, *RINT1*, or *LIV8* display increased sensitivity to potassium cyanide (KCN). Approximately 1 x 10^4 cells were grown for 24 hours in YPAD containing 1 mM KCN. Quantitative plating was used to determine colony

forming units (CFU) before and after KCN treatment. Data is shown as a percentage of starting CFU. Error bars represent the SD. A mutant containing a deletion of the alternative oxidase gene (*aox1Δ*) was used as a positive control for KCN sensitivity.

Figure S8

Growth in low-iron conditions. Serial dilutions of wild-type (WT) and mutant strains were grown on low-iron medium (LIM) plates and low-iron medium plates supplemented with 100 mM $FeCl_3$ and 1 mM ascorbic acid (LIM + iron). A mutant containing a deletion of an iron permease gene (*cft1Δ*) was used as a positive control for decreased growth in low ferrous iron conditions. Asterisks indicate two deletion strains that displayed growth defects on LIM. However, unlike with the *cft1Δ* mutant, these defects were not compensated for by addition of ferrous iron.

Figure S9

Urease assay. Wild-type (WT) and mutant strains were placed in Christensen's urea medium for 24 hours at 37°C to test for urease activity. A pink color indicated an increase in pH due to degradation of urea by urease. A yellow color indicated a lack of urease activity. A *C. neoformans* mutant containing a deletion of the urease gene (*ure1Δ*) was used as a negative control for urease activity. The strain in each well is indicated in the key below. All tested mutants displayed normal urease function.

Figure S10

Virulence phenotypes of *liv6Δ* and *rgd1Δ* during monotypic infection. 8-10 mice per strain were intranasally infected with WT, **(A)** *liv6Δ*, or **(B)** *rgd1Δ*, and progression to the disease endpoint was monitored. Two independent knockout strains were tested for each gene. P-value < 0.001 for all strains.

Figure S11

Quantification of the sizes of capsules shown in Figure 4B. Capsule sizes were measured relative to the diameters of the cells. Capsules from at least 30 cells per strain were measured. Error bars represent the SD.

Figure S12

Antibody staining using a mixture of anti-capsule and anti-beta-glucan antibodies was used to distinguish internalized *C. neoformans* cells from those attached to the exterior of the macrophage. Arrows identify internalized *C. neoformans* cells.

Figure S13

Light sonication prior to incubation with macrophages does not affect viability of *C. neoformans* cells or phagocytosis by macrophages. **(A)** Viability of wild-type (WT) and *gat201Δ* cells before and after light sonication (see Experimental Procedures) was determined by calculating CFU using quantitative serial dilutions of cultures. Post-sonication CFU was compared to pre-sonication CFU. We attribute the increase in CFU after sonication to the separation of clumps of cells in the cultures. **(B)** WT and *gat201Δ*

cells were prepared with and without sonication and incubated with RAW264.7 macrophages as in Figure 5. Sonication did not have any effect on the degree of observed phagocytosis. Error bars represent the SD.

FIGURE S1

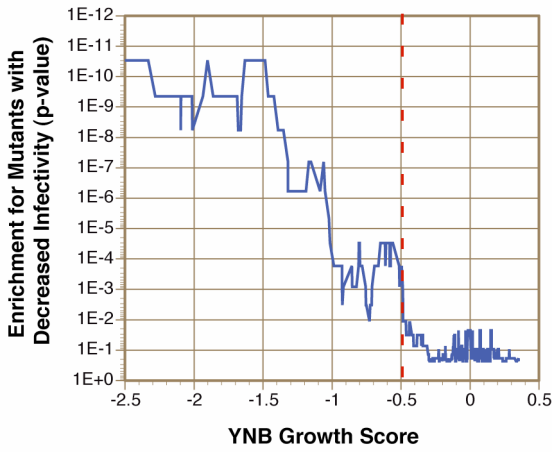
Enrichment for Mutants with Decreased Infectivity (p-value)
1E-12
1E-11
1E-10
1E-9
1E-8
1E-7
1E-6
1E-5
1E-4
1E-3
1E-2
1E-1
1E+0
-2.5
-2
-1.5
-1
-0.5
0
0.5
YNB Growth Score

FIGURE S2

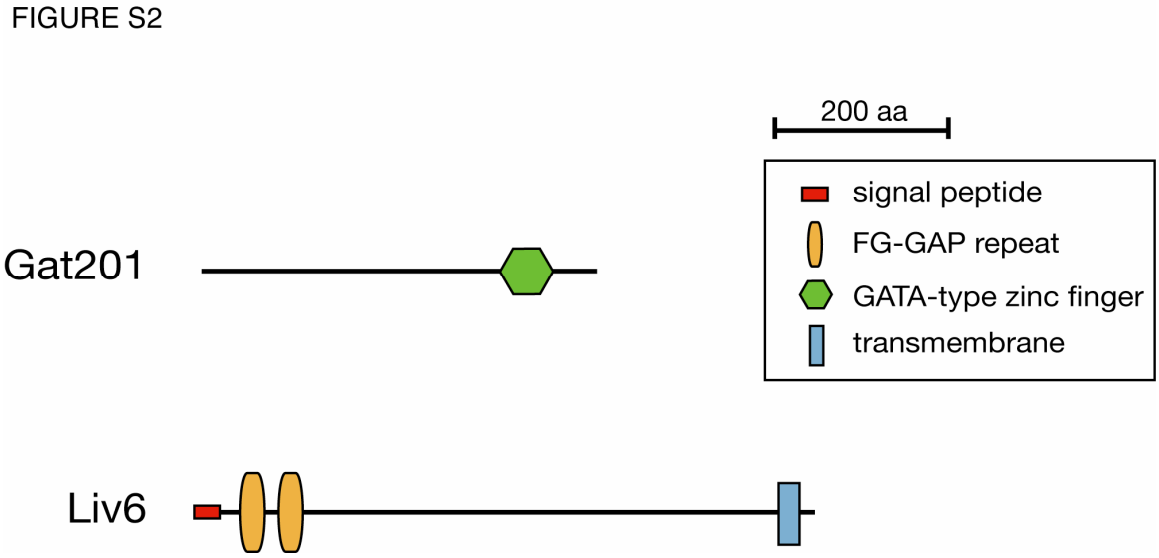
200 aa
signal peptide
FG-GAP repeat
GATA-type zinc finger
transmembrane
Gat201
Liv6

FIGURE S3

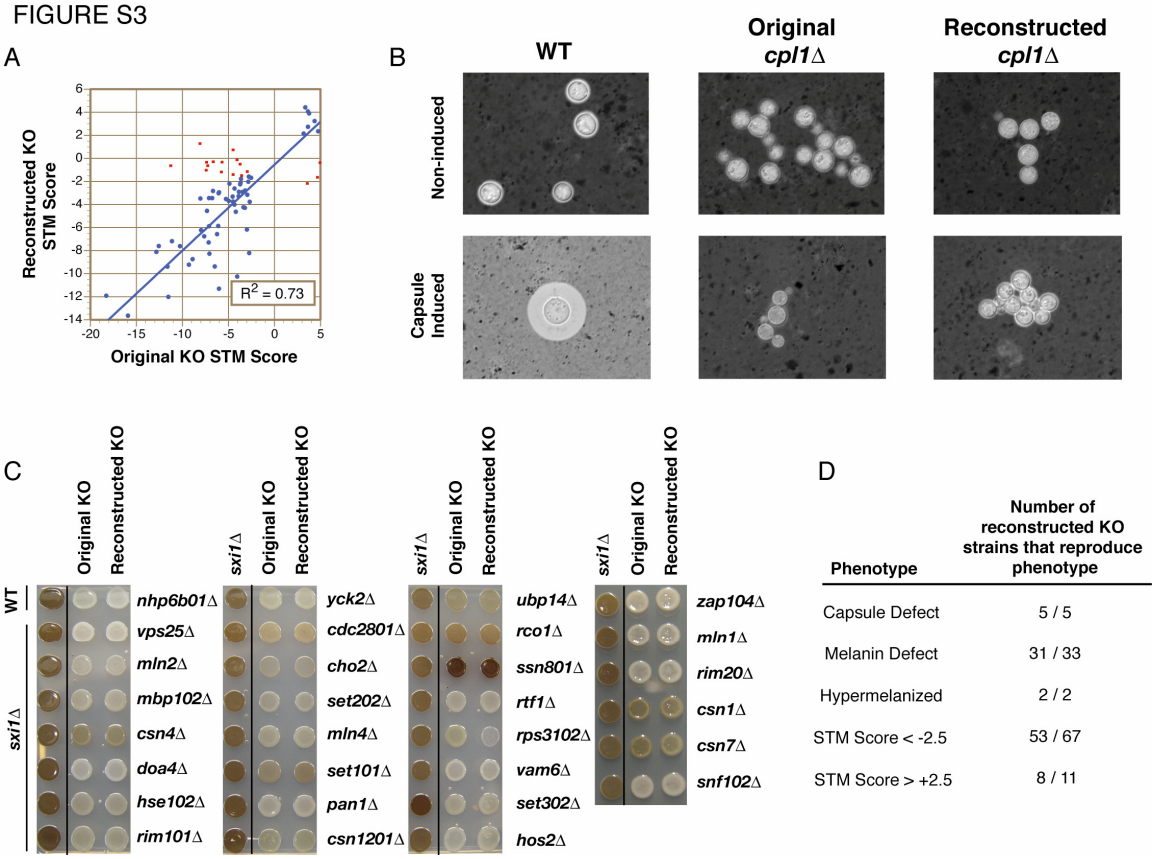

D

Phenotype	Number of reconstructed KO strains that reproduce phenotype
Capsule Defect	5 / 5
Melanin Defect	31 / 33
Hypermelanized	2 / 2
STM Score < -2.5	53 / 67
STM Score > +2.5	8 / 11

FIGURE S4

A

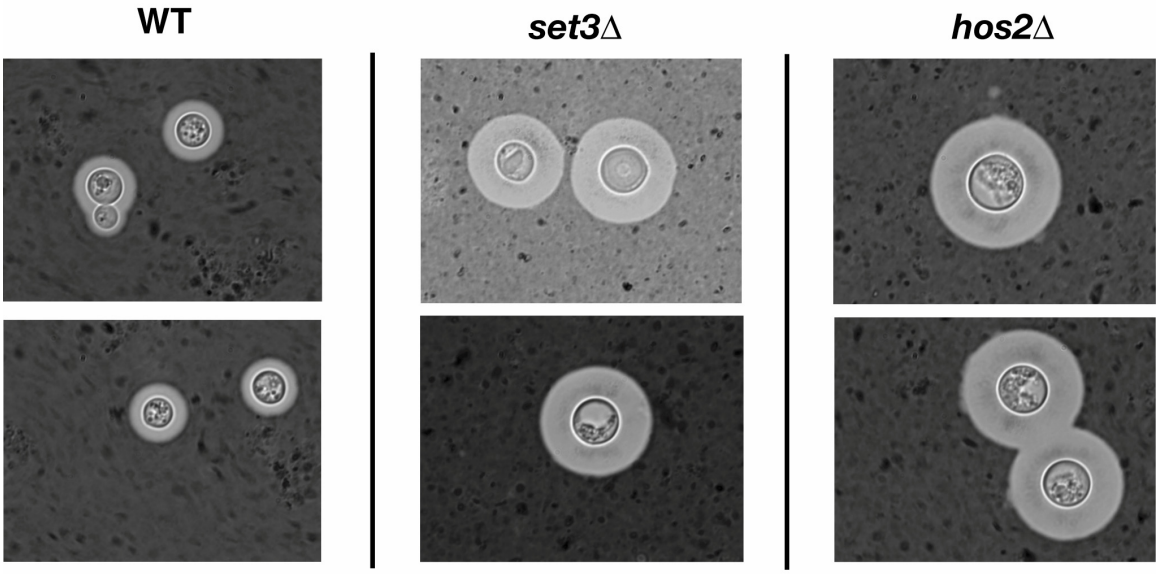
WT
set3Δ
hos2Δ

B

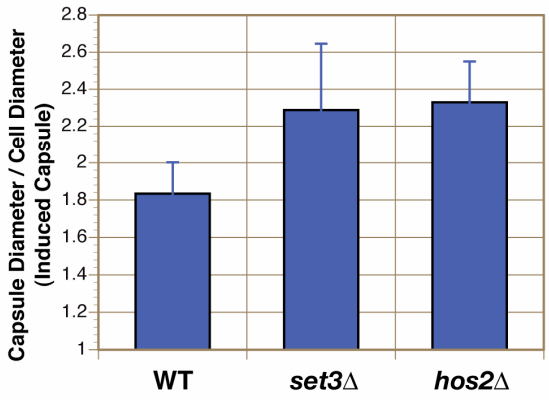
Capsule Diameter / Cell Diameter (Induced Capsule)
2.8
2.6
2.4
2.2
2
1.8
1.6
1.4
1.2
1
WT
set3Δ
hos2Δ

FIGURE S5

A

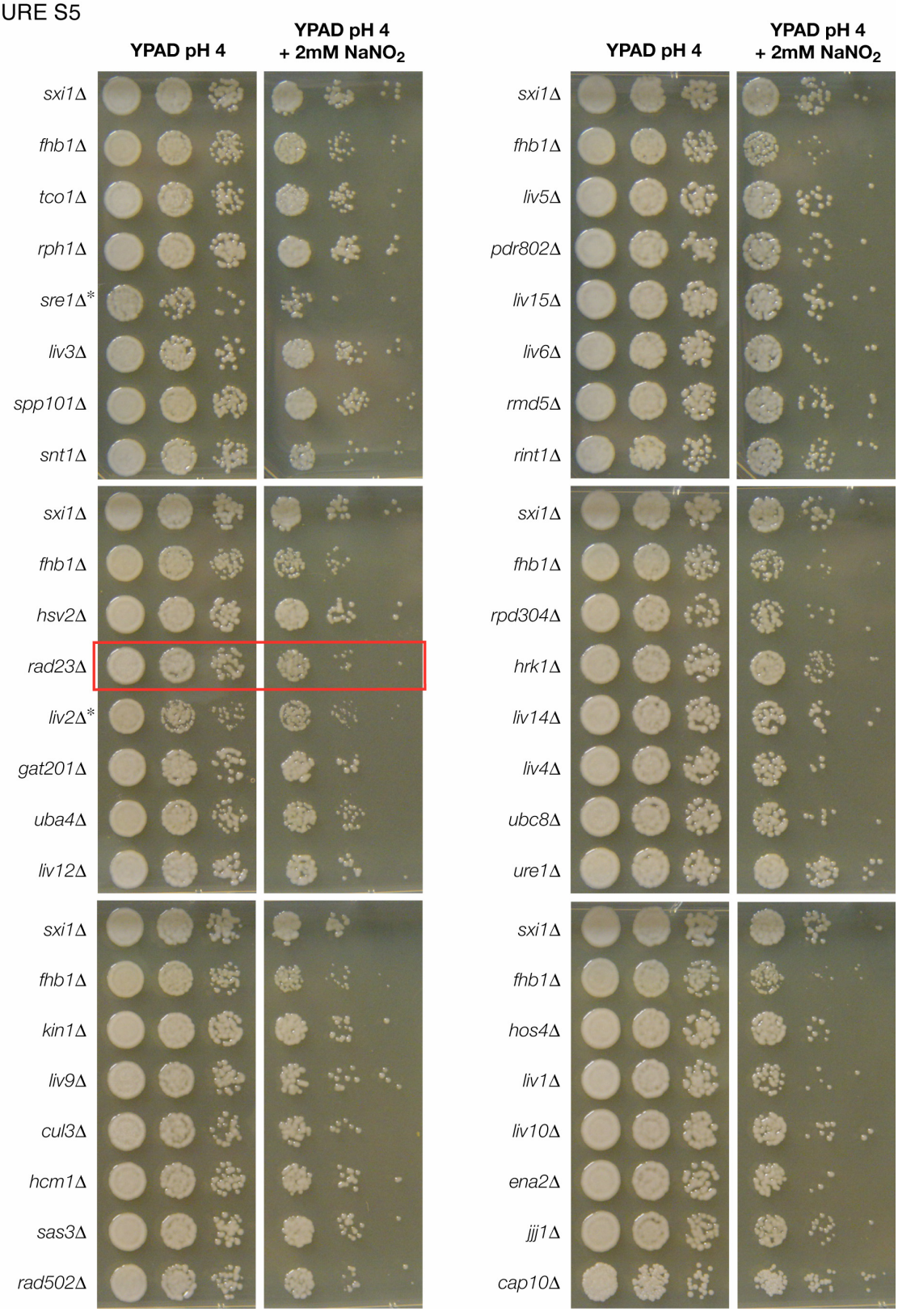
YPAD pH 4
YPAD pH 4 + 2mM $NaNO_2$
sxi1Δ
fhb1Δ
tco1Δ
rph1Δ
sre1Δ*
liv3Δ
spp101Δ
snt1Δ
sxi1Δ
fhb1Δ
hsv2Δ
rad23Δ
liv2Δ*
gat201Δ
uba4Δ
liv12Δ
sxi1Δ
fhb1Δ
kin1Δ
liv9Δ
cul3Δ
hcm1Δ
sas3Δ
rad502Δ
YPAD pH 4
YPAD pH 4 + 2mM $NaNO_2$
sxi1Δ
fhb1Δ
liv5Δ
pdr802Δ
liv15Δ
liv6Δ
rmd5Δ
rint1Δ
sxi1Δ
fhb1Δ
rpd304Δ
hrk1Δ
liv14Δ
liv4Δ
ubc8Δ
ure1Δ
sxi1Δ
fhb1Δ
hos4Δ
liv1Δ
liv10Δ
ena2Δ
jjj1Δ
cap10Δ

FIGURE S5 (cont.)

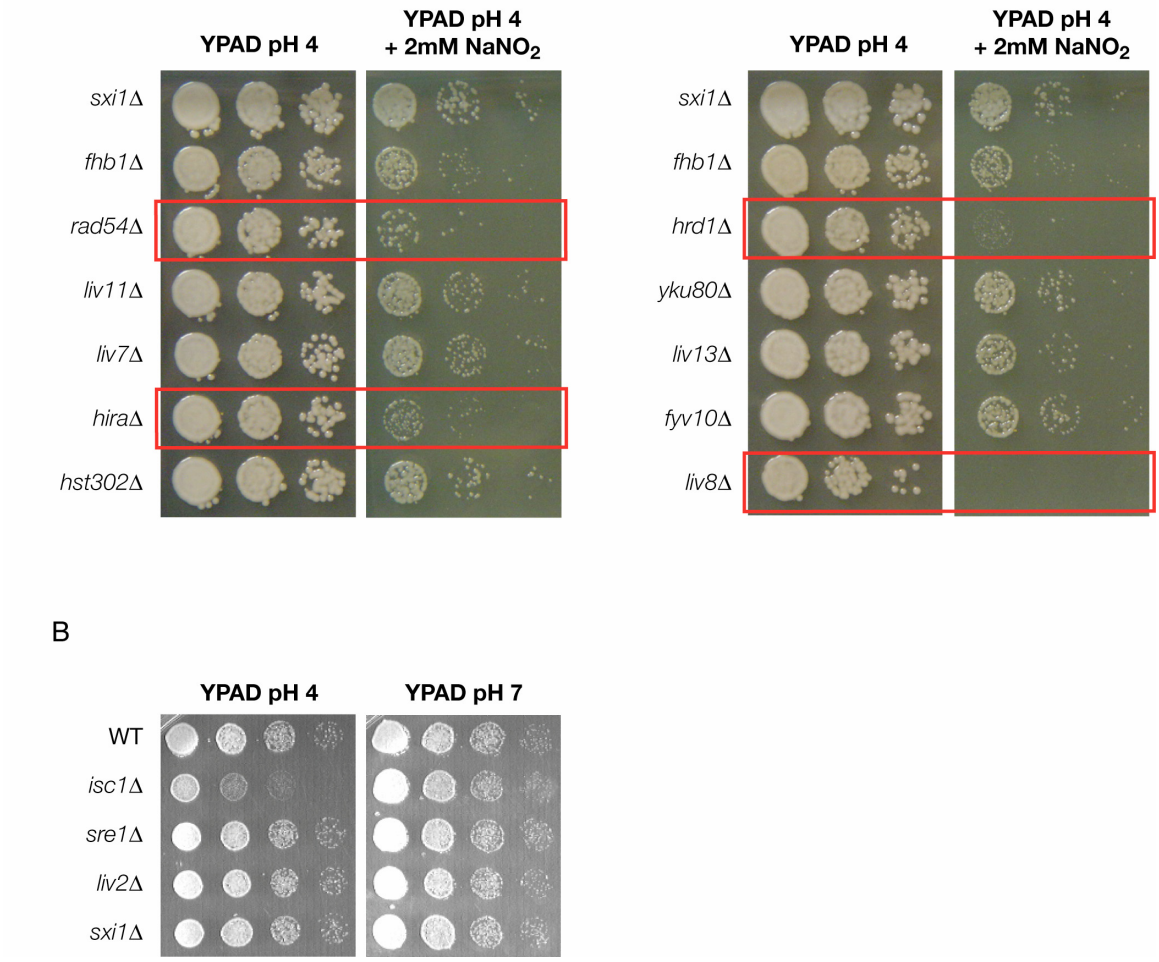

B

FIGURE S6

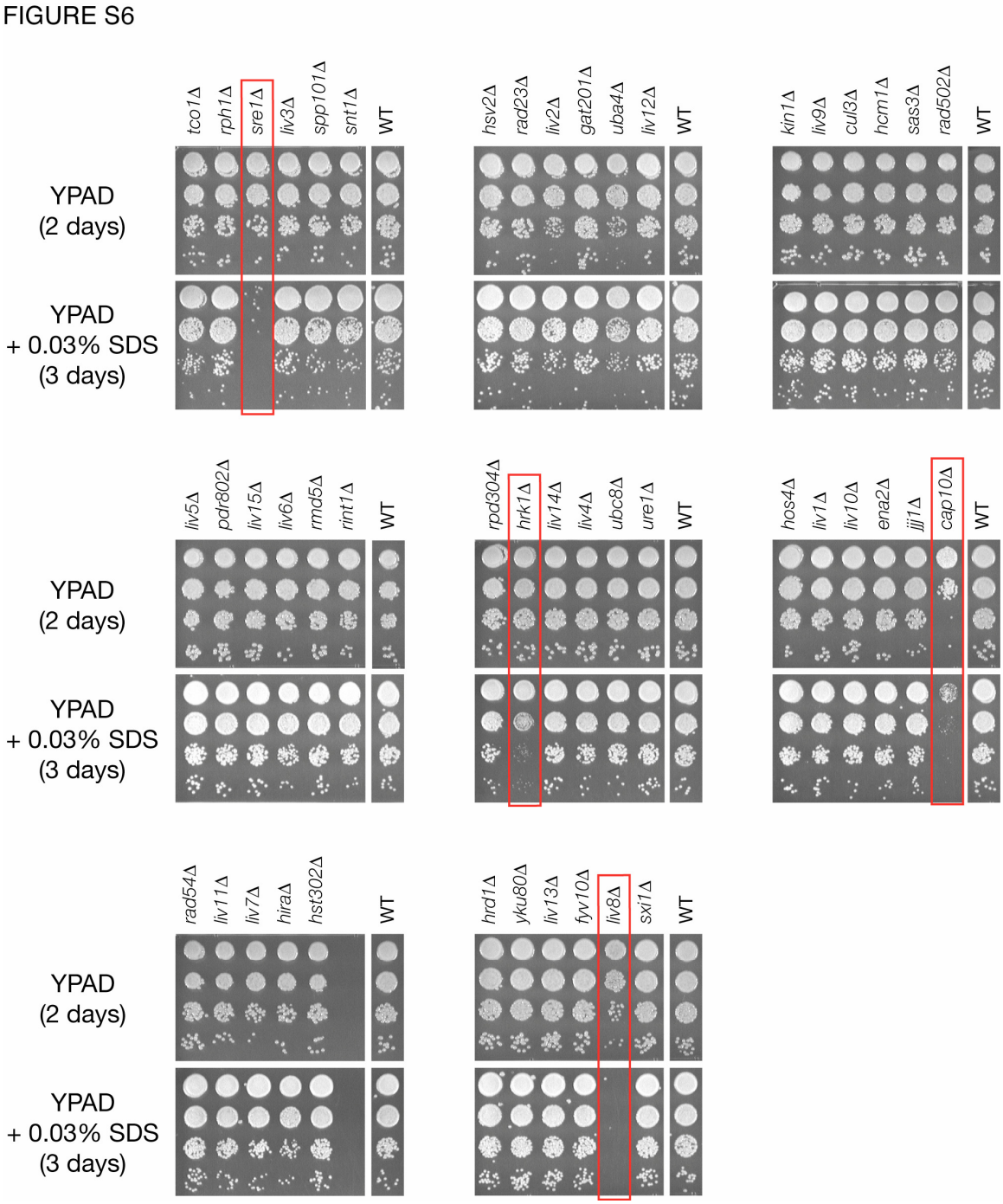
YPAD
(2 days)
YPAD
+ 0.03% SDS
(3 days)
tco1Δ
rph1Δ
sre1Δ
liv3Δ
spp101Δ
snt1Δ
WT
hsv2Δ
rad23Δ
liv2Δ
gat201Δ
uba4Δ
liv12Δ
WT
kin1Δ
liv9Δ
cul3Δ
hcm1Δ
sas3Δ
rad502Δ
WT
liv5Δ
pdr802Δ
liv15Δ
liv6Δ
rmd5Δ
rint1Δ
WT
rpd304Δ
hrk1Δ
liv14Δ
liv4Δ
ubc8Δ
ure1Δ
WT
hos4Δ
liv1Δ
liv10Δ
ena2Δ
jjj1Δ
cap10Δ
WT
rad54Δ
liv11Δ
liv7Δ
hiraΔ
hst302Δ
WT
hrd1Δ
yku80Δ
liv13Δ
fyv10Δ
liv8Δ
sxi1Δ
WT

FIGURE S7

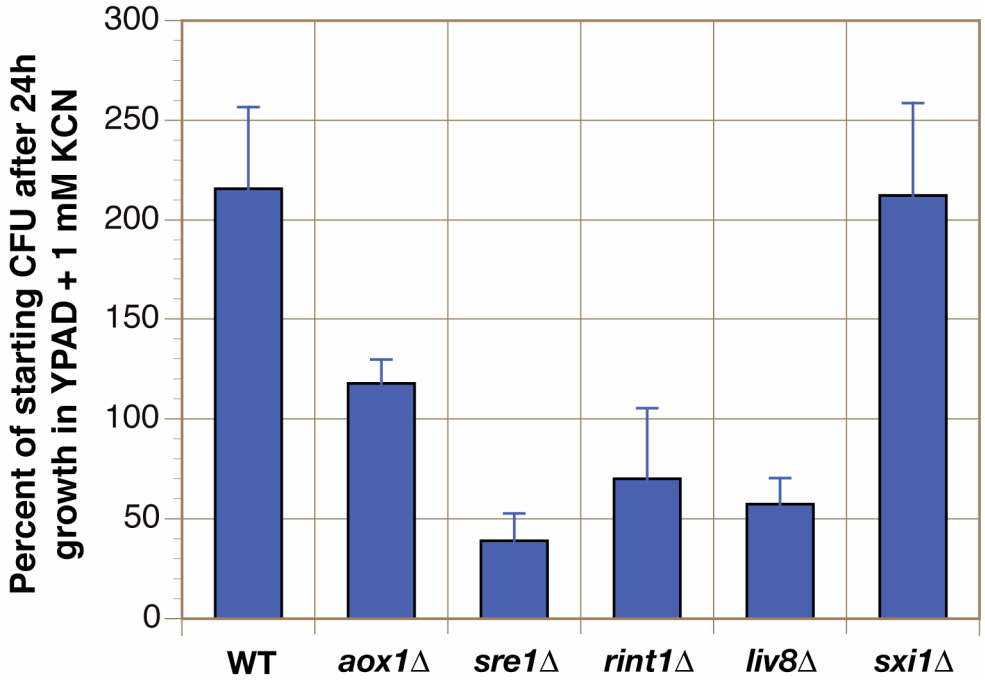
Percent of starting CFU after 24h growth in YPAD + 1 mM KCN
300
250
200
150
100
50
0
WT
aox1Δ
sre1Δ
rint1Δ
liv8Δ
sxi1Δ

FIGURE S8

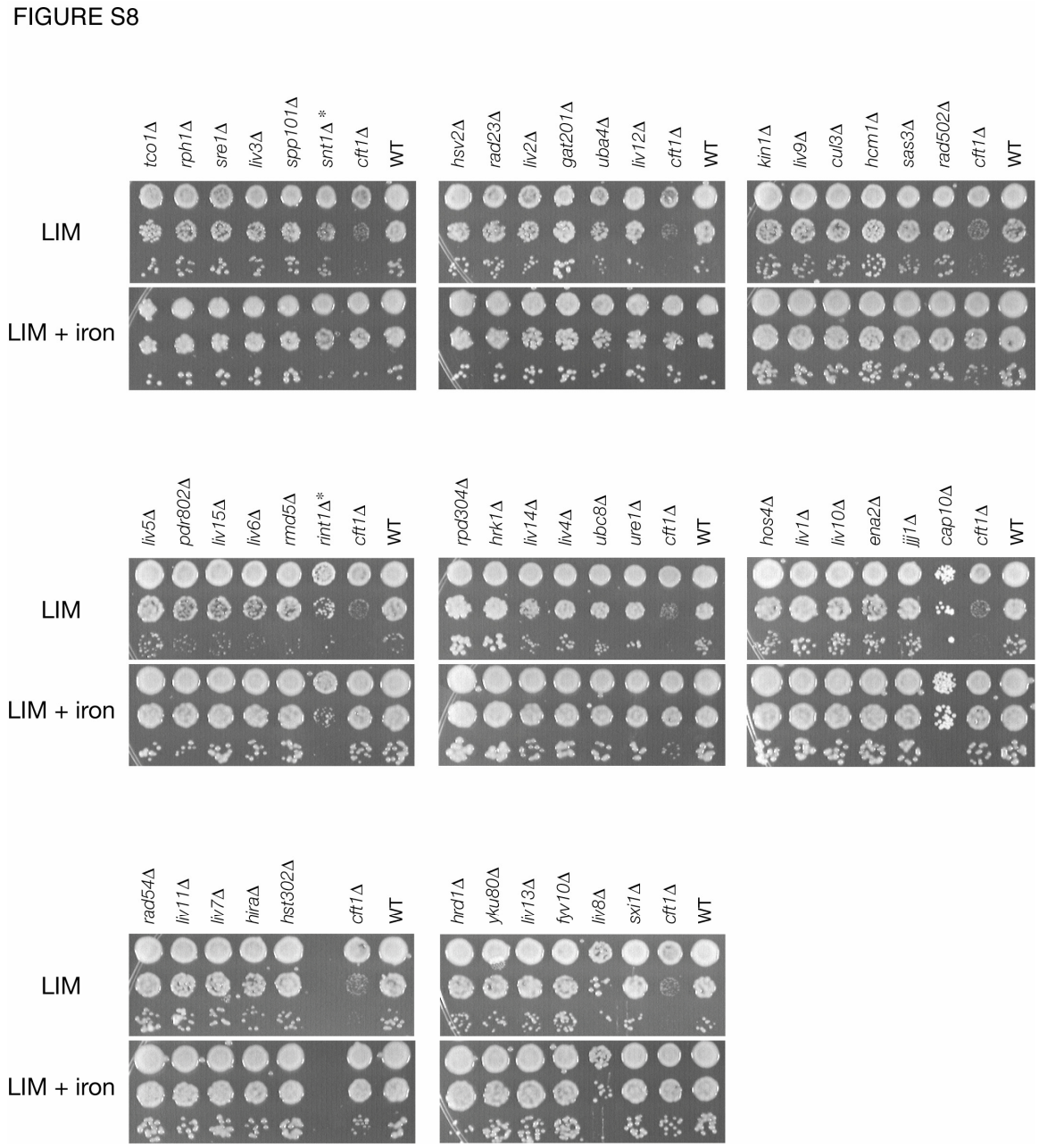
LIM
LIM + iron
tco1Δ
rph1Δ
sre1Δ
liv3Δ
spp101Δ
snt1Δ*
cft1Δ
WT
hsv2Δ
rad23Δ
liv2Δ
gat201Δ
uba4Δ
liv12Δ
cft1Δ
WT
kin1Δ
liv9Δ
cul3Δ
hcm1Δ
sas3Δ
rad502Δ
cft1Δ
WT
liv5Δ
pdr802Δ
liv15Δ
liv6Δ
rmd5Δ
rint1Δ*
cft1Δ
WT
rpd304Δ
hrk1Δ
liv14Δ
liv4Δ
ubc8Δ
ure1Δ
cft1Δ
WT
hos4Δ
liv1Δ
liv10Δ
ena2Δ
jjj1Δ
cap10Δ
cft1Δ
WT
rad54Δ
liv11Δ
liv7Δ
hiraΔ
hst302Δ
cft1Δ
WT
hrd1Δ
yku80Δ
liv13Δ
fyv10Δ
liv8Δ
sxl1Δ
cft1Δ
WT

FIGURE S9

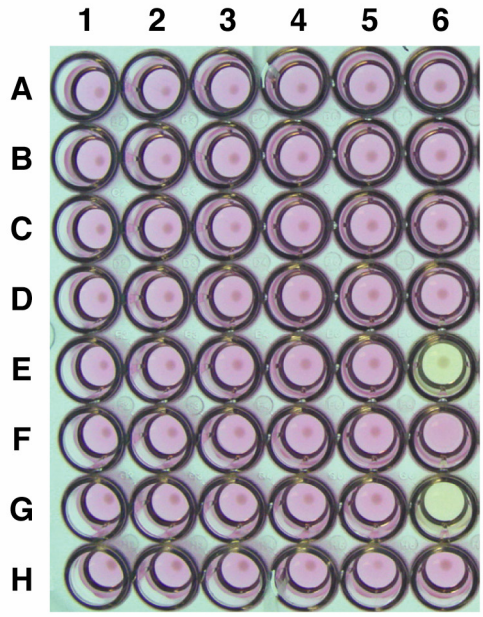

	1	2	3	4	5	6
A	*tco1Δ*	*rph1Δ*	*sre1Δ*	*liv3Δ*	*spp101Δ*	*snt1Δ*
B	*hsv2Δ*	*rad23Δ*	*liv2Δ*	*gat201Δ*	*uba4Δ*	*liv12Δ*
C	*kin1Δ*	*liv9Δ*	*cul3Δ*	*hcm1Δ*	*sas3Δ*	*rad502Δ*
D	*liv5Δ*	*pdr802Δ*	*liv15Δ*	*liv6Δ*	*rmd5Δ*	*rint1Δ*
E	*rpd304Δ*	*hrk1Δ*	*liv14Δ*	*liv4Δ*	*ubc8Δ*	*ure1Δ*
F	*hos4Δ*	*liv1Δ*	*liv10Δ*	*ena2Δ*	*jjj1Δ*	*cap10Δ*
G	*rad54Δ*	*liv11Δ*	*liv7Δ*	*hiraΔ*	*hst302Δ*	empty
H	*hrd1Δ*	*yku80Δ*	*liv13Δ*	*fyv10Δ*	*liv8Δ*	*sxi1Δ*

FIGURE S10

A

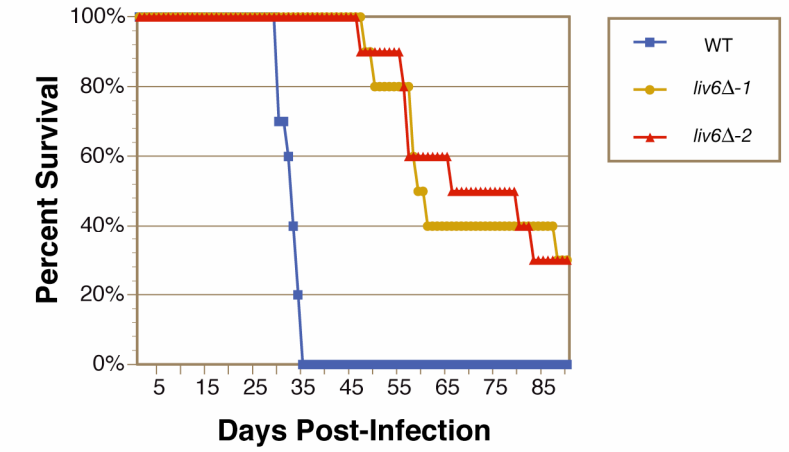

B

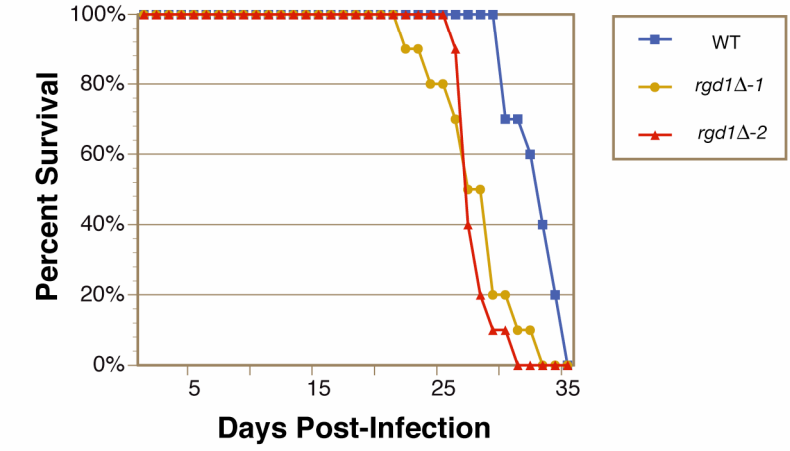

FIGURE S11

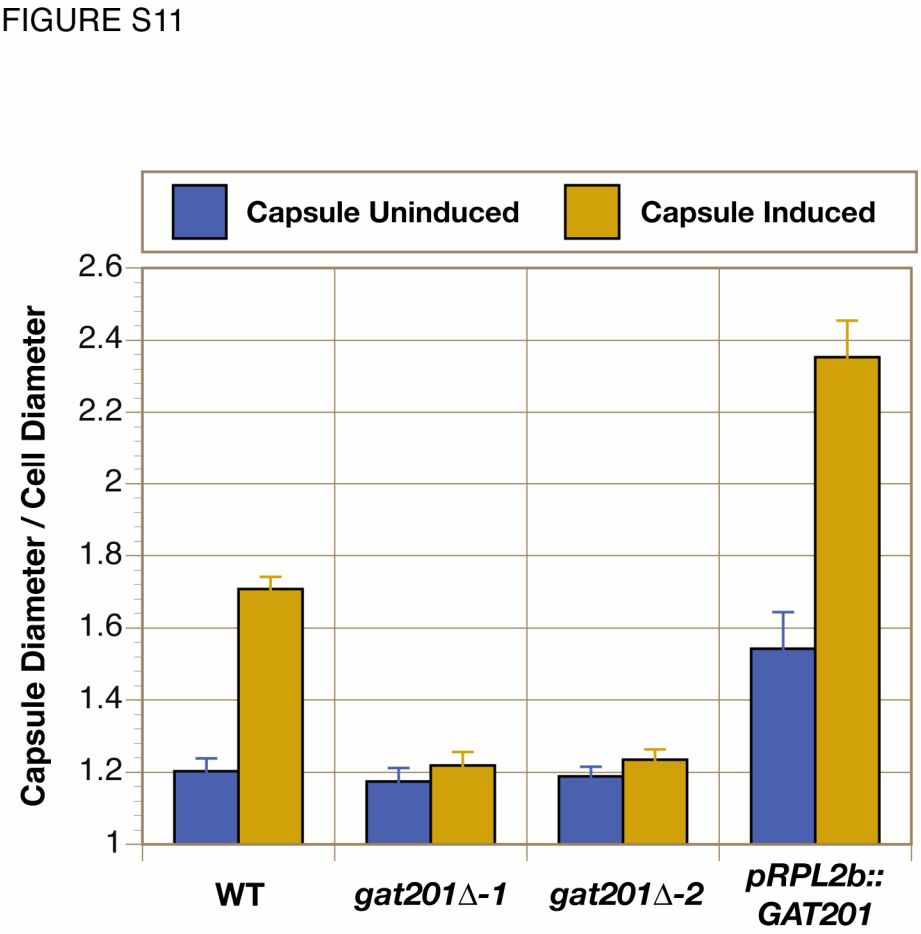
Capsule Uninduced
Capsule Induced
Capsule Diameter / Cell Diameter
2.6
2.4
2.2
2
1.8
1.6
1.4
1.2
1
WT
gat201Δ-1
gat201Δ-2
pRPL2b::
GAT201

FIGURE S12

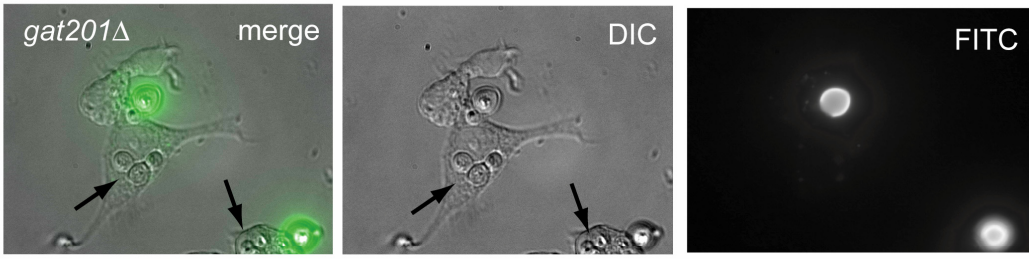

FIGURE S13

A

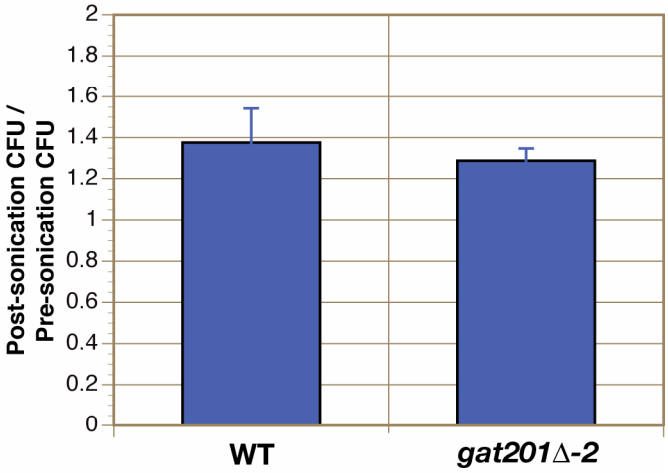

B

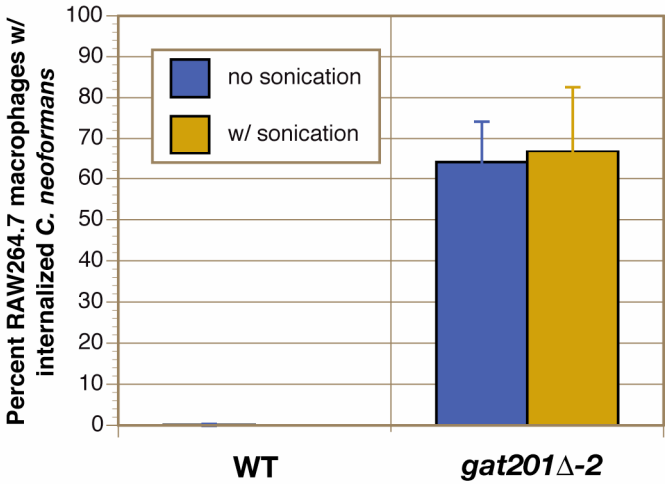

SUPPLEMENTAL TABLES AND LEGENDS

Tables S1 and S3–S7 are provided along with the Supplemental Data as separate Excel files. Table S2 is included below.

Table S1

Summary of targeted gene deletions in *C. neoformans* that have been reported in the literature. Virulence defects may have been determined using various models and routes of infection.

TABLE S2 Phenotypes of previously described virulence mutants determined by systematic phenotyping in this study

KO#	Gene Name	Broad Annotation	Reference	Gene Deletion Phenotype			
				STM Score	Growth Score	Dry Colony	Melanin
Genes known to affect virulence							
D497	*KIN1*	CNAG_01938	Mylonakis et al., 2004	-12.8↓	0.24	+	+
D1002	*MPK1*	CNAG_04514	Kraus et al., 2003	-11.8↓	-1.90↓	+	+
D629	*CAP10*	CNAG_02628	Chang and Kwon-Chung, 1999; Moyrand and Janbon, 2004	-11.6↓	-0.75↓	-	+
D1040	*UGT1*	CNAG_05139	Moyrand et al., 2007	-9.6↓	-6.77↓	+	+
D42	*CAP60*	CNAG_00600	Chang and Kwon-Chung, 1998; Moyrand and Janbon, 2004	-7.4↓	-2.70↓	-	+
D45	*CAP59*	CNAG_00721	Chang and Kwon-Chung, 1994; Moyrand and Janbon, 2004	-7.3↓	-0.66↓	-	+
D1452	*CAS1*	CNAG_06429	Janbon et al., 2001	-7.3↓	-1.15↓	+	+
D355	*PBX1*	CNAG_01172	Liu et al., 2007	-6.6↓	0.13	-	+
D1423	*SCH9*	CNAG_06301	Wang et al., 2004	-6.2↓	0.35	+	+
D792	*SKN7*	CNAG_03409	Bahn et al., 2006; Wormley et al., 2005	-6.0↓	-0.92↓	+	+
D281	*CAS35*	CNAG_00746	Moyrand et al., 2004; Moyrand et al., 2007	-5.7↓	0.40	-	+
D755	*CAC1*	CNAG_03202	Alspaugh et al., 2002	-5.4↓	0.22	+	-
D581	*BWC2*	CNAG_02435	Idnurm and Heitman, 2005	-4.8↓	0.12	+	+
D217	*PKA1*	CNAG_00396	D'Souza et al., 2001	-4.6↓	0.44	+	-
D1209	*SRE1*	CNAG_04804	Chun et al., 2007; Chang et al., 2007	-4.6↓	-0.02	+	+
D1049	*BWC1*	CNAG_05181	Idnurm and Heitman, 2005	-3.8↓	-0.12	+	+
D795	*CTS1*	CNAG_03422	Fox et al., 2003	-3.6↓	-3.60↓	+	+
D679	*CAP64*	CNAG_02855	Chang et al., 1996; Moyrand and Janbon, 2004	-3.5↓	ND	-	+
D476	*TCO1*	CNAG_01850	Bahn et al., 2006; Chun et al., 2007	-3.0↓	-0.11	+	+
D1056	*NRG1*	CNAG_05222	Cramer et al. 2006	-2.6↓	ND	-	+
D291	*CBP1*	CNAG_00802	Fox and Heitman, 2005; Gorlach et al., 2000	-1.9	0.08	+	+
D432	*SCP1*	CNAG_01580	Chun et al., 2007; Chang et al., 2007	-0.8 (-3.6)*	0.06	+	+
D1281	*URE1*	CNAG_05540	Cox et al., 2000	0.4	0.16	+	+
D1127	*LAC1*	CNAG_03464	Noverr et al., 2004	0.5	0.05	+	-
CM146	*LAC1, LAC2*		This study	0.3	ND	+	-
Genes known to not affect virulence							
D739	*CMT1*	CNAG_03158	Sommer et al., 2003	-1.8	-0.30	+	+
D1199	*RAS2*	CNAG_04761	Waugh et al., 2002	-1.6	0.06	+	+
D377	*GPB1*	CNAG_01262	Wang et al., 2000	-0.3	0.09	+	+
D170	*GPA2*	CNAG_00179	Li et al., 2007	0.2	-0.19	+	+
D934	*PKA2*	CNAG_05540	Cox et al., 2000	0.3	0.34	+	+
D522	*GPA3*	CNAG_02090	Li et al., 2007	0.9	-0.08	+	+
D1126	*LAC2*	CNAG_03464	Missall et al., 2005; Pukkla-Worley et al., 2005	1.6	0.04	+	+

Table S2

Genes in the knockout collection that have previously been characterized for virulence. Phenotypes represent those identified in this work. Down arrows (↓) indicate significant decreases compared to wild-type. Asterisks (*) indicate that this mutant was placed in a different pool of mutants and retested by STM. Results of the second assay are in parentheses.

Table S3

Results of systematic *in vivo* and *in vitro* profiling of the deletion collection and reconstructed knockout strains. Melanin and capsule phenotypes were scored qualitatively with negative numbers indicating a defect and positive numbers indicating an enhancement.

Table S4

Deletion strains in the knockout collection.

Table S5

Additional strains used in this study including reconstructed deletion strains.

Table S6

Primers used in this study (not including primers used to create gene deletion strains).

Table S7

Signature tag sequences found in the deletion strains and tag-specific primers used for quantitative PCR**.**

SUPPLEMENTAL EXPERIMENTAL PROCEDURES

Strains and media

Cryptococcus neoformans var. grubii serotype A strain H99 (a gift from Dr. J. K. Lodge) was used as wild-type. Strains were routinely grown in rich medium, YPAD (1% yeast extract, 2% Bacto-peptone, 2% glucose, 0.015% L-tryptophan, 0.004% adenine) or minimal medium, YNB (0.45% Yeast Nitrogen Base w/o amino acids w/o ammonium sulfate, 1.5% ammonium sulfate, 2% glucose).

Generation of Gene Deletion Strains

Targeted regions in the reconstructed knockouts and the double knockout mutants can be found in Table S5 and by entering the gene names at http://cryptogenome.ucsf.edu. Gene deletions were generated using nourseothricin (NAT) resistance (*natR*) cassettes containing signature tag sequences. Constructs were targeted using 1kb flanking regions upstream and downstream of the targeted sequence. The expected 5' recombination event was detected by colony PCR using a primer within the *natR* cassette and a primer outside the 1kb flanking region. Positive transformants were streaked onto YPAD agar plates and single colonies were repatched onto YPAD agar plates containing 100 μg/mL NAT. The expected 3' recombination event was then verified by colony PCR using a primer within the NAT cassette and a primer outside the 1 kb flanking region. Double mutant strains were generated using a neomycin (NEO) resistance cassette (*neoR*) as a second marker as previously described. *CAP10*, *CAP60*, and *CAP64* were deleted in the D429 strain background (*gat201Δ-1*) and *LAC2* was deleted in the D1127 strain background (*lac1Δ*).

Signature-tagged mutagenesis

Groups of 48 *C. neoformans* deletion strains were individually grown in liquid YPAD at 30°C in 96-well deep-pocket plates (Greiner) without shaking for 3 days. 200μL of each culture were combined into a single pool and cells were counted using a hemacytometer. 1 x 10^7 cells were washed twice in PBS and resuspended in 1 mL of PBS. This pooled inoculum was used to infect mice as described below. Three mice were infected per pool. Three aliquots of each inoculum (~5 x 10^5 cells) were also plated on Sabouraud agar plates containing 40 μg/mL gentamicin and 50 μg/mL carbenicillin. The plates were incubated for two days at 30°C. The resulting cells were resuspended in water and lyophilized. Genomic DNA (Input DNA) was purified independently from each plate using hexadecyltrimethyl ammonium bromide (CTAB, Sigma).

Infected mice were monitored and sacrificed as described below. Lungs were removed and homogenized in 5 ml sterile PBS. Serial dilutions of each organ sample were plated on Sabouraud agar plates containing 40 μg/mL gentamicin and 50 μg/mL carbenicillin. The plates were incubated for two days at 30°C and genomic DNA (Output DNA) from each set of lungs was purified as above.

The amounts of each signature tag in a genomic DNA prep were measured using 48 simultaneous quantitative PCR reactions. Each reaction was identical except for a different tag-specific primer (Table S7). SYBR Green dye (Molecular Probes) was used to detect double-stranded DNA and fluorescent signal was measured on an Opticon DNA Engine PCR machine (MJ Research). Melting curves were collected to confirm that only

a single product was produced in the reaction. The threshold cycle (Ct) was determined for each reaction.

To calculate the STM score, a variation of the $2^{-\Delta\Delta Ct}$ method for quantitation analysis was utilized (Livak and Schmittgen, 2001). Specifically, for each input DNA prep, a ΔCt was calculated for each signature tag by comparing to the median Ct value in that set of reactions ($Ct_{median} - Ct_{tag}$). The ΔCt values from three independent input DNA samples were averaged to determine the $\Delta Ct_{tag\text{-}input}$. Next, for each output DNA prep, a $\Delta Ct_{tag\text{-}mouse}$ was calculated for each signature tag by comparing to the median Ct value in that set of reactions ($Ct_{median} - Ct_{tag}$). The STM score of each mutant after infection in a given mouse was then calculated as the ΔΔCt ($\Delta Ct_{tag\text{-}mouse} - \Delta Ct_{tag\text{-}input}$). STM scores from three mice were averaged to determine a final STM score for each mutant.

Animal studies

Pooled inocula for STM infections were prepared as described above. For monotypic infections, *C. neoformans* strains were grown in liquid YPAD cultures overnight at 30°C. Cells were counted using a hemacytometer and 1×10^7 cells were washed twice in PBS and resuspended in 1 mL of PBS. 5-6 week-old female A/J (NCI) mice were anesthetized by intraperitoneal injection of ketamine (75 mg/kg) and medetomidine (0.5-1.0 mg/kg). The mice were then suspended from a silk thread by their front incisors and 50μL of the inoculum (5×10^5 cells) were slowly pipetted into the nares. After 10 minutes, the mice were lowered and the anesthesia was reversed by intraperitoneal injection of atipamezole (1.0-2.5 mg/kg). For survival curves, 8-10 mice were infected per inoculum. The concentrations of the inocula were confirmed by plating

serial dilutions. Mice were monitored several times a week until onset of symptoms (weight loss, ruffled fur, abnormal gait) and then monitored daily. Mice that displayed signs of severe morbidity (weight loss, abnormal gait, hunched posture, ruffled fur, swelling of the cranium) were sacrificed by CO_2 inhalation followed by cervical dislocation. The lungs were harvested as described above for STM analysis. This protocol was reviewed and approved by the UCSF Institutional Animal Care and Use Committee.

Polysaccharide capsule

To induce polysaccharide capsule formation, *C. neoformans* strains were grown in Sabouraud medium overnight at 30°C. The cultures were then diluted 1/100 in either Sabouraud medium (non-inducing conditions) or 10% Sabouraud medium buffered to pH 7.3 with 50 mM MOPS (capsule-inducing conditions) and grown at 30°C for two days. 5μL of India ink was added to 20μL of culture and the capsule was visualized using bright-field microscopy at 160x magnification using an Axiovert 200M (Zeiss) microscope running Axiovision software. To quantify capsule size, the cell diameter and capsule diameter of at least 30 cells per strain per condition were measured.

For antibody staining of the capsule, a previously described mouse monoclonal antibody (mAb339) specific for the main capsule polysaccharide, glucoronoxylomannan, was used (Belay et al., 1997). *C. neoformans* strains were grown in liquid YNB medium overnight at 30°C. $1x10^7$ cells from each culture were washed three times with PBS, resuspended in 1 mL DMEM, and cultured at 37° with 5% CO_2 in 24-well tissue culture plates (BD Biosciences). After 24 hours, the cells were collected and washed twice with PBS. The cells were then incubated with mAb 339 for 1 hour at 37°, then washed twice

with PBS prior to incubation with FITC-conjugated donkey anti-mouse secondary antibody (Jackson ImmunoResearch) for 1 hour at room temperature in the dark. The cells were then washed twice with PBS, resuspended in PBS and placed on a microscope slide. The cells were visualized using an Axiovert 200M (Zeiss) microscope running Axiovision software (exposure times for the FITC channel ranged from 350-400 ms).

Melanin

Cultures grown to saturation in YPAD medium were spotted onto melanin-inducing plates containing 100 mg/mL L-DOPA (L-dihydroxyphenylalanine, Sigma) and grown at 30°C. Accumulation of pigment was observed over 2-3 days.

Growth in YNB

Groups of 48 *C. neoformans* deletion strains were individually grown in liquid YPAD at 30°C in 96-well deep-pocket plates (Greiner) without shaking for 3 days. Cultures were then diluted 1/50 in 800μL of YNB prewarmed to 37°C using a Multimek automated pipettor (Beckman). An aliquot of 200μL was removed to measure the starting OD_{600} using an optical plate reader (Molecular Devices). Plates were grown at 37°C with shaking at 1000 rpm for 24 hours in a Multitron shaker-incubator (Infors). An aliquot of 200μL was removed to measure the finishing OD_{600}. The amount of growth was measured as $(OD_{24h} - OD_{0h})/OD_{0h} - 1$. A growth score was calculated for each mutant by normalizing to the median growth in that group of 48 mutants as follows: Growth score = $\log_2(growth_{mutant} / growth_{median})$.

Additional Phenotyping

For growth on pH 4 medium and sensitivity to nitric oxide, cultures were grown to saturation in YPAD at 30°C in 96-well deep-pocket plates (Greiner) without shaking and serial dilutions were plated on pH 4 YPAD agar plates (pH adjusted using 25 mM succinic acid) and pH 4 YPAD agar plates containing 2 mM $NaNO_2$. pH 7 YPAD agar plates were made using 25 mM MOPS buffer. For growth on SDS, cultures were grown to saturation in YPAD at 30°C in 96-well deep-pocket plates without shaking and serial dilutions were plated on YPAD agar plates and YPAD containing 0.03% SDS. For growth on low ferrous iron media, cultures were first grown in 96-well deep-pocket plates without shaking in low iron medium (LIM, Zaragoza and Casadevall, 2004) for two days to deplete intracellular stores of iron. Serial dilutions were then plated on 0.5x LIM agar plates and on 0.5x LIM agar plates supplemented with 100 mM $FeCl_3$ and 1 mM ascorbic acid. Ascorbic acid reduces ferric iron in the medium to ferrous iron.

For growth in potassium cyanide (KCN), an initial screen of mutants was performed by growing cultures to saturation in YPAD at 30°C in 96-well deep-pocket plates without shaking, transferring approximately 1 x 10^4 cells to 600 μL of YPAD containing 1 mM KCN, and incubating the cultures at 30°C for 24 hours. Serial dilutions of both the starting cultures and the KCN-treated cultures were pinned onto YPAD plates and relative colony counts were determined by estimating the number of colonies in a given spot. Mutants that demonstrated potential sensitivity to KCN were retested using more precise quantitative plating of serial dilutions. Mutants identified using this approach are shown in Figure S7.

To measure urease activity, cultures were grown to saturation in YPAD at 30°C in 96-well deep-pocket plates without shaking and diluted 1:10 in Christensen's urea medium (5g NaCl, 2g KH2PO4, 1g glucose, 1g peptone, 0.012g phenol red, 20g urea in 1L water, pH 6.8). Reactions were kept at 37°C for 24 hours and monitored for a change in color from yellow to pink, indicating an increase in pH due to the degradation of urea.

GAT201 overexpression

To overexpress *GAT201*, the promoter of the ribosomal gene *RPL2b* was inserted upstream of the endogenous *GAT201* coding sequence. Insertion of the *pRPL2b* sequence was performed by biolistically transforming H99 with two linear DNA constructs simultaneously. The first targeted the *pRPL2b* sequence for insertion just upstream of the *GAT201* start codon but did not contain any selection marker. The second targeted the *natR* cassette for insertion upstream of the *pRPL2b* sequence and downstream of the *pGAT201* sequence. Thus, the proper targeting of the *natR* cassette requires the insertion of the *pRPL2b* sequence upstream of the *GAT201* sequence. Both constructs were generated using overlap fusion PCR. Overexpression of the *GAT201* transcript was verified by quantitative RT-QPCR as described previously (Chow et al., 2007) and microarray analysis (Figure 4).

RAW264.7 cells

RAW264.7 murine macrophages were maintained in feeding media consisting of Dulbecco's modified Eagle's medium (DMEM) supplemented with 10% heat-inactivated

fetal bovine serum, 20mM HEPES, and 2mM glutamine (UCSF Cell Culture Facility) and cultured at 37°C, 5% CO_2. Macrophages were used between passages 4-15.

Assignment of gene function

Description of gene functions in this work were assigned using several approaches. First, the predicted protein domains encoded by genes (using Pfam, SMART, and SignalP algorithms) provided by the Broad Institute, by an annotation database (http://cryptogenome.ucsf.edu), and by direct submission (http://pfam.janelia.org/, http://smart.embl-heidelberg.de/, and http://www.cbs.dtu.dk/services/SignalP/) were used to assign putative function. Second, BLASTX data available at http://cryptogenome.ucsf.edu were used to identify proteins in the non-redundant database with strong homology to predicted *C. neoformans* proteins. Finally, this annotation database previously identified the best BLASTX hit for a given *C. neoformans* gene model in the genomes of nine ascomycetes (*Saccharomyces cerevisiae*, *Schizosaccharomyces pombe*, *Neurospora crassa*, *Candida albicans*, *Aspergillus fumigatus*, *Aspergillus nidulans*, *Coccidiodes immitis*, *Fusarium gaminearum*, and *Magnaporthe grisea*) and two basidiomycetes (*Ustilago maydis* and *Phanerochaete chrysosporium*) (Chow et al., 2007). Gene models that did not have BLASTX hits with expect values < 0.001 in any of the other genomes were termed *C. neoformans*-specific.

SUPPLEMENTAL REFERENCES

Akhter, S., McDade, H. C., Gorlach, J. M., Heinrich, G., Cox, G. M., and Perfect, J. R. (2003). Role of alternative oxidase gene in pathogenesis of Cryptococcus neoformans. Infect Immun *71*, 5794-5802.

Alspaugh, J. A., Cavallo, L. M., Perfect, J. R., and Heitman, J. (2000). RAS1 regulates filamentation, mating and growth at high temperature of Cryptococcus neoformans. Mol Microbiol *36*, 352-365.

Alspaugh, J. A., Perfect, J. R., and Heitman, J. (1997). Cryptococcus neoformans mating and virulence are regulated by the G-protein alpha subunit GPA1 and cAMP. Genes Dev *11*, 3206-3217.

Alspaugh, J. A., Pukkila-Worley, R., Harashima, T., Cavallo, L. M., Funnell, D., Cox, G. M., Perfect, J. R., Kronstad, J. W., and Heitman, J. (2002). Adenylyl cyclase functions downstream of the Galpha protein Gpa1 and controls mating and pathogenicity of Cryptococcus neoformans. Eukaryot Cell *1*, 75-84.

Bahn, Y. S., Cox, G. M., Perfect, J. R., and Heitman, J. (2005a). Carbonic anhydrase and CO2 sensing during Cryptococcus neoformans growth, differentiation, and virulence. Curr Biol *15*, 2013-2020.

Bahn, Y. S., Geunes-Boyer, S., and Heitman, J. (2007). Ssk2 mitogen-activated protein kinase kinase kinase governs divergent patterns of the stress-activated Hog1 signaling pathway in Cryptococcus neoformans. Eukaryot Cell *6*, 2278-2289.

Bahn, Y. S., Hicks, J. K., Giles, S. S., Cox, G. M., and Heitman, J. (2004). Adenylyl cyclase-associated protein Aca1 regulates virulence and differentiation of Cryptococcus neoformans via the cyclic AMP-protein kinase A cascade. Eukaryot Cell *3*, 1476-1491.

Bahn, Y. S., Kojima, K., Cox, G. M., and Heitman, J. (2005b). Specialization of the HOG pathway and its impact on differentiation and virulence of Cryptococcus neoformans. Mol Biol Cell *16*, 2285-2300.

Bahn, Y. S., Kojima, K., Cox, G. M., and Heitman, J. (2006). A unique fungal two-component system regulates stress responses, drug sensitivity, sexual development, and virulence of Cryptococcus neoformans. Mol Biol Cell *17*, 3122-3135.

Baker, L. G., Specht, C. A., Donlin, M. J., and Lodge, J. K. (2007). Chitosan, the deacetylated form of chitin, is necessary for cell wall integrity in Cryptococcus neoformans. Eukaryot Cell *6*, 855-867.

Banks, I. R., Specht, C. A., Donlin, M. J., Gerik, K. J., Levitz, S. M., and Lodge, J. K. (2005). A chitin synthase and its regulator protein are critical for chitosan production and growth of the fungal pathogen Cryptococcus neoformans. Eukaryot Cell *4*, 1902-1912.

Chang, Y. C., Bien, C. M., Lee, H., Espenshade, P. J., and Kwon-Chung, K. J. (2007). Sre1p, a regulator of oxygen sensing and sterol homeostasis, is required for virulence in Cryptococcus neoformans. Mol Microbiol *64*, 614-629.

Chang, Y. C., Jong, A., Huang, S., Zerfas, P., and Kwon-Chung, K. J. (2006). CPS1, a homolog of the Streptococcus pneumoniae type 3 polysaccharide synthase gene, is important for the pathobiology of Cryptococcus neoformans. Infect Immun *74*, 3930-3938.

Chang, Y. C., and Kwon-Chung, K. J. (1994). Complementation of a capsule-deficient mutation of Cryptococcus neoformans restores its virulence. Mol Cell Biol *14*, 4912-4919.

Chang, Y. C., and Kwon-Chung, K. J. (1998). Isolation of the third capsule-associated gene, CAP60, required for virulence in Cryptococcus neoformans. Infect Immun *66*, 2230-2236.

Chang, Y. C., and Kwon-Chung, K. J. (1999). Isolation, characterization, and localization of a capsule-associated gene, CAP10, of Cryptococcus neoformans. J Bacteriol *181*, 5636-5643.

Chang, Y. C., Miller, G. F., and Kwon-Chung, K. J. (2003). Importance of a developmentally regulated pheromone receptor of Cryptococcus neoformans for virulence. Infect Immun *71*, 4953-4960.

Chang, Y. C., Penoyer, L. A., and Kwon-Chung, K. J. (1996). The second capsule gene of cryptococcus neoformans, CAP64, is essential for virulence. Infect Immun *64*, 1977-1983.

Chikamori, M., and Fukushima, K. (2005). A new hexose transporter from Cryptococcus neoformans: molecular cloning and structural and functional characterization. Fungal Genet Biol *42*, 646-655.

Chun, C. D., Liu, O. W., and Madhani, H. D. (2007). A link between virulence and homeostatic responses to hypoxia during infection by the human fungal pathogen Cryptococcus neoformans. PLoS Pathog *3*, e22.

Coe, J. G., Wilson, C. F., Sorrell, T. C., Latouche, N. G., and Wright, L. C. (2003). Cloning of CnLYSO1, a novel extracellular lysophospholipase of the pathogenic fungus Cryptococcus neoformans. Gene *316*, 67-78.

Cottrell, T. R., Griffith, C. L., Liu, H., Nenninger, A. A., and Doering, T. L. (2007). The pathogenic fungus Cryptococcus neoformans expresses two functional GDP-mannose transporters with distinct expression patterns and roles in capsule synthesis. Eukaryot Cell *6*, 776-785.

Cox, G. M., Harrison, T. S., McDade, H. C., Taborda, C. P., Heinrich, G., Casadevall, A., and Perfect, J. R. (2003). Superoxide dismutase influences the virulence of Cryptococcus neoformans by affecting growth within macrophages. Infect Immun *71*, 173-180.

Cox, G. M., McDade, H. C., Chen, S. C., Tucker, S. C., Gottfredsson, M., Wright, L. C., Sorrell, T. C., Leidich, S. D., Casadevall, A., Ghannoum, M. A., and Perfect, J. R. (2001). Extracellular phospholipase activity is a virulence factor for Cryptococcus neoformans. Mol Microbiol *39*, 166-175.

Cox, G. M., Mukherjee, J., Cole, G. T., Casadevall, A., and Perfect, J. R. (2000). Urease as a virulence factor in experimental cryptococcosis. Infect Immun *68*, 443-448.

Cramer, K. L., Gerrald, Q. D., Nichols, C. B., Price, M. S., and Alspaugh, J. A. (2006). Transcription factor Nrg1 mediates capsule formation, stress response, and pathogenesis in Cryptococcus neoformans. Eukaryot Cell *5*, 1147-1156.

Cruz, M. C., Cavallo, L. M., Gorlach, J. M., Cox, G., Perfect, J. R., Cardenas, M. E., and Heitman, J. (1999). Rapamycin antifungal action is mediated via conserved complexes with FKBP12 and TOR kinase homologs in Cryptococcus neoformans. Mol Cell Biol *19*, 4101-4112.

D'Souza, C. A., Alspaugh, J. A., Yue, C., Harashima, T., Cox, G. M., Perfect, J. R., and Heitman, J. (2001). Cyclic AMP-dependent protein kinase controls virulence of the fungal pathogen Cryptococcus neoformans. Mol Cell Biol *21*, 3179-3191.

Davidson, R. C., Nichols, C. B., Cox, G. M., Perfect, J. R., and Heitman, J. (2003). A MAP kinase cascade composed of cell type specific and non-specific elements controls mating and differentiation of the fungal pathogen Cryptococcus neoformans. Mol Microbiol *49*, 469-485.

de Jesus-Berrios, M., Liu, L., Nussbaum, J. C., Cox, G. M., Stamler, J. S., and Heitman, J. (2003). Enzymes that counteract nitrosative stress promote fungal virulence. Curr Biol *13*, 1963-1968.

Ekena, J. L., Stanton, B. C., Schiebe-Owens, J. A., and Hull, C. M. (2008). Sexual development in Cryptococcus neoformans requires CLP1, a target of the homeodomain transcription factors Sxi1alpha and Sxi2a. Eukaryot Cell *7*, 49-57.

Erickson, T., Liu, L., Gueyikian, A., Zhu, X., Gibbons, J., and Williamson, P. R. (2001). Multiple virulence factors of Cryptococcus neoformans are dependent on VPH1. Mol Microbiol *42*, 1121-1131.

Fan, W., Idnurm, A., Breger, J., Mylonakis, E., and Heitman, J. (2007). Eca1, a sarcoplasmic/endoplasmic reticulum Ca2+-ATPase, is involved in stress tolerance and virulence in Cryptococcus neoformans. Infect Immun *75*, 3394-3405.

Fox, D. S., Cox, G. M., and Heitman, J. (2003). Phospholipid-binding protein Cts1 controls septation and functions coordinately with calcineurin in Cryptococcus neoformans. Eukaryot Cell *2*, 1025-1035.

Fox, D. S., Cruz, M. C., Sia, R. A., Ke, H., Cox, G. M., Cardenas, M. E., and Heitman, J. (2001). Calcineurin regulatory subunit is essential for virulence and mediates interactions with FKBP12-FK506 in Cryptococcus neoformans. Mol Microbiol *39*, 835-849.

Fox, D. S., and Heitman, J. (2005). Calcineurin-binding protein Cbp1 directs the specificity of calcineurin-dependent hyphal elongation during mating in Cryptococcus neoformans. Eukaryot Cell *4*, 1526-1538.

Gerik, K. J., Donlin, M. J., Soto, C. E., Banks, A. M., Banks, I. R., Maligie, M. A., Selitrennikoff, C. P., and Lodge, J. K. (2005). Cell wall integrity is dependent on the PKC1 signal transduction pathway in Cryptococcus neoformans. Mol Microbiol *58*, 393-408.

Giles, S. S., Batinic-Haberle, I., Perfect, J. R., and Cox, G. M. (2005). Cryptococcus neoformans mitochondrial superoxide dismutase: an essential link between antioxidant function and high-temperature growth. Eukaryot Cell *4*, 46-54.

Giles, S. S., Stajich, J. E., Nichols, C., Gerrald, Q. D., Alspaugh, J. A., Dietrich, F., and Perfect, J. R. (2006). The Cryptococcus neoformans catalase gene family and its role in antioxidant defense. Eukaryot Cell *5*, 1447-1459.

Goins, C. L., Gerik, K. J., and Lodge, J. K. (2006). Improvements to gene deletion in the fungal pathogen Cryptococcus neoformans: absence of Ku proteins increases homologous recombination, and co-transformation of independent DNA molecules allows rapid complementation of deletion phenotypes. Fungal Genet Biol *43*, 531-544.

Gorlach, J., Fox, D. S., Cutler, N. S., Cox, G. M., Perfect, J. R., and Heitman, J. (2000). Identification and characterization of a highly conserved calcineurin binding protein, CBP1/calcipressin, in Cryptococcus neoformans. Embo J *19*, 3618-3629.

Griffith, C. L., Klutts, J. S., Zhang, L., Levery, S. B., and Doering, T. L. (2004). UDP-glucose dehydrogenase plays multiple roles in the biology of the pathogenic fungus Cryptococcus neoformans. J Biol Chem *279*, 51669-51676.

Heung, L. J., Kaiser, A. E., Luberto, C., and Del Poeta, M. (2005). The role and mechanism of diacylglycerol-protein kinase C1 signaling in melanogenesis by Cryptococcus neoformans. J Biol Chem *280*, 28547-28555.

Hicks, J. K., Bahn, Y. S., and Heitman, J. (2005). Pde1 phosphodiesterase modulates cyclic AMP levels through a protein kinase A-mediated negative feedback loop in Cryptococcus neoformans. Eukaryot Cell *4*, 1971-1981.

Hicks, J. K., D'Souza, C. A., Cox, G. M., and Heitman, J. (2004). Cyclic AMP-dependent protein kinase catalytic subunits have divergent roles in virulence factor production in two varieties of the fungal pathogen Cryptococcus neoformans. Eukaryot Cell *3*, 14-26.

Hsueh, Y. P., and Shen, W. C. (2005). A homolog of Ste6, the a-factor transporter in Saccharomyces cerevisiae, is required for mating but not for monokaryotic fruiting in Cryptococcus neoformans. Eukaryot Cell *4*, 147-155.

Hu, G., Hacham, M., Waterman, S. R., Panepinto, J., Shin, S., Liu, X., Gibbons, J., Valyi-Nagy, T., Obara, K., Jaffe, H. A.*, et al.* (2008). PI3K signaling of autophagy is required for starvation tolerance and virulenceof Cryptococcus neoformans. J Clin Invest *118*, 1186-1197.

Hull, C. M., Boily, M. J., and Heitman, J. (2005). Sex-specific homeodomain proteins Sxi1alpha and Sxi2a coordinately regulate sexual development in Cryptococcus neoformans. Eukaryot Cell *4*, 526-535.

Hull, C. M., Cox, G. M., and Heitman, J. (2004). The alpha-specific cell identity factor Sxi1alpha is not required for virulence of Cryptococcus neoformans. Infect Immun *72*, 3643-3645.

Idnurm, A., Giles, S. S., Perfect, J. R., and Heitman, J. (2007). Peroxisome function regulates growth on glucose in the basidiomycete fungus Cryptococcus neoformans. Eukaryot Cell *6*, 60-72.

Idnurm, A., and Heitman, J. (2005). Light controls growth and development via a conserved pathway in the fungal kingdom. PLoS Biol *3*, e95.

Janbon, G., Himmelreich, U., Moyrand, F., Improvisi, L., and Dromer, F. (2001). Cas1p is a membrane protein necessary for the O-acetylation of the Cryptococcus neoformans capsular polysaccharide. Mol Microbiol *42*, 453-467.

Jung, W. H., Sham, A., Lian, T., Singh, A., Kosman, D. J., and Kronstad, J. W. (2008). Iron Source Preference and Regulation of Iron Uptake in Cryptococcus neoformans. PLoS Pathog *4*, e45.

Jung, W. H., Sham, A., White, R., and Kronstad, J. W. (2006). Iron regulation of the major virulence factors in the AIDS-associated pathogen Cryptococcus neoformans. PLoS Biol *4*, e410.

Kingsbury, J. M., Yang, Z., Ganous, T. M., Cox, G. M., and McCusker, J. H. (2004). Cryptococcus neoformans Ilv2p confers resistance to sulfometuron methyl and is required for survival at 37 degrees C and in vivo. Microbiology *150*, 1547-1558.

Kraus, P. R., Fox, D. S., Cox, G. M., and Heitman, J. (2003). The Cryptococcus neoformans MAP kinase Mpk1 regulates cell integrity in response to antifungal drugs and loss of calcineurin function. Mol Microbiol *48*, 1377-1387.

Lee, H., Chang, Y. C., and Kwon-Chung, K. J. (2005). TUP1 disruption reveals biological differences between MATa and MATalpha strains of Cryptococcus neoformans. Mol Microbiol *55*, 1222-1232.

Lee, H., Chang, Y. C., Nardone, G., and Kwon-Chung, K. J. (2007). TUP1 disruption in Cryptococcus neoformans uncovers a peptide-mediated density-dependent growth phenomenon that mimics quorum sensing. Mol Microbiol *64*, 591-601.

Li, L., Shen, G., Zhang, Z. G., Wang, Y. L., Thompson, J. K., and Wang, P. (2007). Canonical heterotrimeric G proteins regulating mating and virulence of Cryptococcus neoformans. Mol Biol Cell *18*, 4201-4209.

Liu, M., Du, P., Heinrich, G., Cox, G. M., and Gelli, A. (2006). Cch1 mediates calcium entry in Cryptococcus neoformans and is essential in low-calcium environments. Eukaryot Cell *5*, 1788-1796.

Liu, O. W., Kelly, M. J., Chow, E. D., and Madhani, H. D. (2007). Parallel beta-helix proteins required for accurate capsule polysaccharide synthesis and virulence in the yeast Cryptococcus neoformans. Eukaryot Cell *6*, 630-640.

Luberto, C., Martinez-Marino, B., Taraskiewicz, D., Bolanos, B., Chitano, P., Toffaletti, D. L., Cox, G. M., Perfect, J. R., Hannun, Y. A., Balish, E., and Del Poeta, M. (2003). Identification of App1 as a regulator of phagocytosis and virulence of Cryptococcus neoformans. J Clin Invest *112*, 1080-1094.

Mare, L., Iatta, R., Montagna, M. T., Luberto, C., and Del Poeta, M. (2005). APP1 transcription is regulated by inositol-phosphorylceramide synthase 1-diacylglycerol pathway and is controlled by ATF2 transcription factor in Cryptococcus neoformans. J Biol Chem *280*, 36055-36064.

Missall, T. A., and Lodge, J. K. (2005). Function of the thioredoxin proteins in Cryptococcus neoformans during stress or virulence and regulation by putative transcriptional modulators. Mol Microbiol *57*, 847-858.

Missall, T. A., Moran, J. M., Corbett, J. A., and Lodge, J. K. (2005). Distinct stress responses of two functional laccases in Cryptococcus neoformans are revealed in the absence of the thiol-specific antioxidant Tsa1. Eukaryot Cell *4*, 202-208.

Missall, T. A., Pusateri, M. E., Donlin, M. J., Chambers, K. T., Corbett, J. A., and Lodge, J. K. (2006). Posttranslational, Translational, and Transcriptional Responses to Nitric Oxide Stress in Cryptococcus neoformans: Implications for Virulence. Eukaryot Cell *5*, 518-529.

Missall, T. A., Pusateri, M. E., and Lodge, J. K. (2004). Thiol peroxidase is critical for virulence and resistance to nitric oxide and peroxide in the fungal pathogen, Cryptococcus neoformans. Mol Microbiol *51*, 1447-1458.

Mogensen, E. G., Janbon, G., Chaloupka, J., Steegborn, C., Fu, M. S., Moyrand, F., Klengel, T., Pearson, D. S., Geeves, M. A., Buck, J.*, et al.* (2006). Cryptococcus neoformans senses CO2 through the carbonic anhydrase Can2 and the adenylyl cyclase Cac1. Eukaryot Cell *5*, 103-111.

Moyrand, F., Chang, Y. C., Himmelreich, U., Kwon-Chung, K. J., and Janbon, G. (2004). Cas3p belongs to a seven-member family of capsule structure designer proteins. Eukaryot Cell *3*, 1513-1524.

Moyrand, F., Fontaine, T., and Janbon, G. (2007). Systematic capsule gene disruption reveals the central role of galactose metabolism on Cryptococcus neoformans virulence. Mol Microbiol *64*, 771-781.

Moyrand, F., and Janbon, G. (2004). UGD1, encoding the Cryptococcus neoformans UDP-glucose dehydrogenase, is essential for growth at 37 degrees C and for capsule biosynthesis. Eukaryot Cell *3*, 1601-1608.

Moyrand, F., Klaproth, B., Himmelreich, U., Dromer, F., and Janbon, G. (2002). Isolation and characterization of capsule structure mutant strains of Cryptococcus neoformans. Mol Microbiol *45*, 837-849.

Mylonakis, E., Idnurm, A., Moreno, R., El Khoury, J., Rottman, J. B., Ausubel, F. M., Heitman, J., and Calderwood, S. B. (2004). Cryptococcus neoformans Kin1 protein kinase homologue, identified through a Caenorhabditis elegans screen, promotes virulence in mammals. Mol Microbiol *54*, 407-419.

Nichols, C. B., Perfect, Z. H., and Alspaugh, J. A. (2007). A Ras1-Cdc24 signal transduction pathway mediates thermotolerance in the fungal pathogen Cryptococcus neoformans. Mol Microbiol *63*, 1118-1130.

Noverr, M. C., Williamson, P. R., Fajardo, R. S., and Huffnagle, G. B. (2004). CNLAC1 is required for extrapulmonary dissemination of Cryptococcus neoformans but not pulmonary persistence. Infect Immun *72*, 1693-1699.

Nyhus, K. J., Ozaki, L. S., and Jacobson, E. S. (2002). Role of mitochondrial carrier protein Mrs3/4 in iron acquisition and oxidative stress resistance of Cryptococcus neoformans. Med Mycol *40*, 581-591.

Odom, A., Muir, S., Lim, E., Toffaletti, D. L., Perfect, J., and Heitman, J. (1997). Calcineurin is required for virulence of Cryptococcus neoformans. Embo J *16*, 2576-2589.

Olson, G. M., Fox, D. S., Wang, P., Alspaugh, J. A., and Buchanan, K. L. (2007). Role of protein O-mannosyltransferase Pmt4 in the morphogenesis and virulence of Cryptococcus neoformans. Eukaryot Cell *6*, 222-234.

Panepinto, J., Liu, L., Ramos, J., Zhu, X., Valyi-Nagy, T., Eksi, S., Fu, J., Jaffe, H. A., Wickes, B., and Williamson, P. R. (2005). The DEAD-box RNA helicase Vad1 regulates multiple virulence-associated genes in Cryptococcus neoformans. J Clin Invest *115*, 632-641.

Panepinto, J. C., Komperda, K. W., Hacham, M., Shin, S., Liu, X., and Williamson, P. R. (2007). Binding of serum mannan binding lectin to a cell integrity-defective Cryptococcus neoformans ccr4Delta mutant. Infect Immun *75*, 4769-4779.

Pascon, R. C., Ganous, T. M., Kingsbury, J. M., Cox, G. M., and McCusker, J. H. (2004). Cryptococcus neoformans methionine synthase: expression analysis and requirement for virulence. Microbiology *150*, 3013-3023.

Petzold, E. W., Himmelreich, U., Mylonakis, E., Rude, T., Toffaletti, D., Cox, G. M., Miller, J. L., and Perfect, J. R. (2006). Characterization and regulation of the trehalose synthesis pathway and its importance in the pathogenicity of Cryptococcus neoformans. Infect Immun *74*, 5877-5887.

Pukkila-Worley, R., Gerrald, Q. D., Kraus, P. R., Boily, M. J., Davis, M. J., Giles, S. S., Cox, G. M., Heitman, J., and Alspaugh, J. A. (2005). Transcriptional network of multiple capsule and melanin genes governed by the Cryptococcus neoformans cyclic AMP cascade. Eukaryot Cell *4*, 190-201.

Reese, A. J., Yoneda, A., Breger, J. A., Beauvais, A., Liu, H., Griffith, C. L., Bose, I., Kim, M. J., Skau, C., Yang, S.*, et al.* (2007). Loss of cell wall alpha(1-3) glucan affects Cryptococcus neoformans from ultrastructure to virulence. Mol Microbiol *63*, 1385-1398.

Ren, P., Rossettini, A., Chaturvedi, V., and Hanes, S. D. (2005). The Ess1 prolyl isomerase is dispensable for growth but required for virulence in Cryptococcus neoformans. Microbiology *151*, 1593-1605.

Rittershaus, P. C., Kechichian, T. B., Allegood, J. C., Merrill, A. H., Jr., Hennig, M., Luberto, C., and Del Poeta, M. (2006). Glucosylceramide synthase is an essential regulator of pathogenicity of Cryptococcus neoformans. J Clin Invest *116*, 1651-1659.

Rude, T. H., Toffaletti, D. L., Cox, G. M., and Perfect, J. R. (2002). Relationship of the glyoxylate pathway to the pathogenesis of Cryptococcus neoformans. Infect Immun *70*, 5684-5694.

Rutherford, J. C., Lin, X., Nielsen, K., and Heitman, J. (2008). Amt2 permease is required to induce ammonium-responsive invasive growth and mating in Cryptococcus neoformans. Eukaryot Cell *7*, 237-246.

Sanguinetti, M., Posteraro, B., La Sorda, M., Torelli, R., Fiori, B., Santangelo, R., Delogu, G., and Fadda, G. (2006). Role of AFR1, an ABC transporter-encoding gene, in the in vivo response to fluconazole and virulence of Cryptococcus neoformans. Infect Immun *74*, 1352-1359.

Shea, J. M., Kechichian, T. B., Luberto, C., and Del Poeta, M. (2006). The cryptococcal enzyme inositol phosphosphingolipid-phospholipase C confers resistance to the antifungal effects of macrophages and promotes fungal dissemination to the central nervous system. Infect Immun *74*, 5977-5988.

Sommer, U., Liu, H., and Doering, T. L. (2003). An alpha-1,3-mannosyltransferase of Cryptococcus neoformans. J Biol Chem *278*, 47724-47730.

Tang, R. J., Breger, J., Idnurm, A., Gerik, K. J., Lodge, J. K., Heitman, J., Calderwood, S. B., and Mylonakis, E. (2005). Cryptococcus neoformans gene involved in mammalian pathogenesis identified by a Caenorhabditis elegans progeny-based approach. Infect Immun *73*, 8219-8225.

Tangen, K. L., Jung, W. H., Sham, A. P., Lian, T., and Kronstad, J. W. (2007). The iron- and cAMP-regulated gene SIT1 influences ferrioxamine B utilization, melanization and cell wall structure in Cryptococcus neoformans. Microbiology *153*, 29-41.

Vallim, M. A., Nichols, C. B., Fernandes, L., Cramer, K. L., and Alspaugh, J. A. (2005). A Rac homolog functions downstream of Ras1 to control hyphal differentiation and high-temperature growth in the pathogenic fungus Cryptococcus neoformans. Eukaryot Cell *4*, 1066-1078.

Varma, A., Wu, S., Guo, N., Liao, W., Lu, G., Li, A., Hu, Y., Bulmer, G., and Kwon-Chung, K. J. (2006). Identification of a novel gene, URE2, that functionally complements a urease-negative clinical strain of Cryptococcus neoformans. Microbiology *152*, 3723-3731.

Walton, F. J., Heitman, J., and Idnurm, A. (2006). Conserved elements of the RAM signaling pathway establish cell polarity in the basidiomycete Cryptococcus neoformans in a divergent fashion from other fungi. Mol Biol Cell *17*, 3768-3780.

Walton, F. J., Idnurm, A., and Heitman, J. (2005). Novel gene functions required for melanization of the human pathogen Cryptococcus neoformans. Mol Microbiol *57*, 1381-1396.

Wang, P., Cardenas, M. E., Cox, G. M., Perfect, J. R., and Heitman, J. (2001). Two cyclophilin A homologs with shared and distinct functions important for growth and virulence of Cryptococcus neoformans. EMBO Rep *2*, 511-518.

Wang, P., Cox, G. M., and Heitman, J. (2004a). A Sch9 protein kinase homologue controlling virulence independently of the cAMP pathway in Cryptococcus neoformans. Curr Genet *46*, 247-255.

Wang, P., Cutler, J., King, J., and Palmer, D. (2004b). Mutation of the regulator of G protein signaling Crg1 increases virulence in Cryptococcus neoformans. Eukaryot Cell *3*, 1028-1035.

Wang, P., Nichols, C. B., Lengeler, K. B., Cardenas, M. E., Cox, G. M., Perfect, J. R., and Heitman, J. (2002). Mating-type-specific and nonspecific PAK kinases play shared and divergent roles in Cryptococcus neoformans. Eukaryot Cell *1*, 257-272.

Wang, P., Perfect, J. R., and Heitman, J. (2000). The G-protein beta subunit GPB1 is required for mating and haploid fruiting in Cryptococcus neoformans. Mol Cell Biol *20*, 352-362.

Waterman, S. R., Hacham, M., Hu, G., Zhu, X., Park, Y. D., Shin, S., Panepinto, J., Valyi-Nagy, T., Beam, C., Husain, S.*, et al.* (2007). Role of a CUF1/CTR4 copper regulatory axis in the virulence of Cryptococcus neoformans. J Clin Invest *117*, 794-802.

Waugh, M. S., Nichols, C. B., DeCesare, C. M., Cox, G. M., Heitman, J., and Alspaugh, J. A. (2002). Ras1 and Ras2 contribute shared and unique roles in physiology and virulence of Cryptococcus neoformans. Microbiology *148*, 191-201.

Wills, E. A., Roberts, I. S., Del Poeta, M., Rivera, J., Casadevall, A., Cox, G. M., and Perfect, J. R. (2001). Identification and characterization of the Cryptococcus neoformans phosphomannose isomerase-encoding gene, MAN1, and its impact on pathogenicity. Mol Microbiol *40*, 610-620.

Wormley, F. L., Jr., Heinrich, G., Miller, J. L., Perfect, J. R., and Cox, G. M. (2005). Identification and characterization of an SKN7 homologue in Cryptococcus neoformans. Infect Immun *73*, 5022-5030.

Xue, C., Bahn, Y. S., Cox, G. M., and Heitman, J. (2006). G protein-coupled receptor Gpr4 senses amino acids and activates the cAMP-PKA pathway in Cryptococcus neoformans. Mol Biol Cell *17*, 667-679.

Yang, Z., Pascon, R. C., Alspaugh, A., Cox, G. M., and McCusker, J. H. (2002). Molecular and genetic analysis of the Cryptococcus neoformans MET3 gene and a met3 mutant. Microbiology *148*, 2617-2625.

Yoneda, A., and Doering, T. L. (2006). A Eukaryotic Capsular Polysaccharide Is Synthesized Intracellularly and Secreted Via Exocytosis. Mol Biol Cell.

Zaragoza, O., and Casadevall, A. (2004). Experimental modulation of capsule size in Cryptococcus neoformans. Biol Proced Online *6*, 10-15.

Zhang, S., Hacham, M., Panepinto, J., Hu, G., Shin, S., Zhu, X., and Williamson, P. R. (2006). The Hsp70 member, Ssa1, acts as a DNA-binding transcriptional co-activator of laccase in Cryptococcus neoformans. Mol Microbiol *62*, 1090-1101.

Zhu, X., and Williamson, P. R. (2003). A CLC-type chloride channel gene is required for laccase activity and virulence in Cryptococcus neoformans. Mol Microbiol *50*, 1271-1281.